

pH-RESPONSIVE INTERPENETRATING POLYMER NETWORK HYDROGEL  
 MICROBEADS OF POLYACRYLAMIDE-G-GUM KONDAGOGU AND  
 SODIUM ALGINATE FOR GASTROPROTECTIVE DRUG DELIVERY: *IN*  
*VITRO-IN VIVO* CHARACTERIZATIONS

GOPAL SALUNKHE,\* SOPAN NANGARE,\*\* PRATIKSHA DEVKAR,\* KETAN PATIL,\*  
 PIYUSH BAFNA\*\*\* and LAXMIKANT ZAWAR\*

\*Department of Pharmaceutics, H. R. Patel Institute of Pharmaceutical Education and Research, Shirpur  
 425405, Maharashtra State, India

\*\*Department of Pharmaceutical Chemistry, H. R. Patel Institute of Pharmaceutical Education and  
 Research, Shirpur 425405, Maharashtra State, India

\*\*\*Department of Pharmacology, H. R. Patel Institute of Pharmaceutical Education and Research, Shirpur  
 425405, Maharashtra State, India

✉ Corresponding author: L. R. Zawar, shwet.zawar@gmail.com

Received April 5, 2024

The present work aims to design interpenetrating polymer network (IPN) mediated hydrogel microbeads of hydrolyzed polyacrylamide-g-gum kondagogu (H-pAAM-g-GK) and sodium alginate (SA) for pH-sensitive gastroprotective drug delivery of diclofenac sodium (DS). In brief, the pAAM-g-GK was prepared using microwave irradiation, followed by conversion into a pH-sensitive polymer (H-pAAM-g-GK) using alkaline hydrolysis. Then, DS-loaded IPN microbeads were made utilizing an ionotropic gelation method using  $\text{Ca}^{+2}$  ions and glutaraldehyde (GA) as a crosslinking agent. After this, different characterizations, such as FT-IR, DSC, PXRD, swelling analysis, drug entrapment, drug release study, *in vivo* anti-inflammatory activity, *etc.*, were performed. The amorphous state of DS in the microbeads was validated by thermograms and diffractograms, whereas SEM analysis confirmed the spherical shape of the obtained DS-loaded H-pAAM-g-GK@SA mediated microbeads. The pulsatile swelling analysis assured the H-pAAM-g-GK@SA mediated microbeads showed significantly increased swelling as the pH switched from 1.2 to 7.4. Additionally, the microbeads exhibit a 15% DS release in a pH 1.2 buffer medium, while a substantial 94% of the drug was released in a pH 7.4 buffer. It assured the DS release was drastically augmented as the pH of the surrounding medium was switched from acidic to alkaline. Principally, the COOH- groups of hydrogels offer ionization at higher pH levels, wherein the osmotic pressure within the microbeads rises, resulting in more swelling and higher drug release. Finally, the *in vivo* anti-inflammatory activity assured pH-sensitive sustained release of DS. In conclusion, the H-pAAM-g-GK@SA mediated pH-sensitive IPN hydrogel microbeads show potential in the design of gastroprotective oral delivery systems for DS. In the future, H-pAAM-g-GK can be used for the design of pH-sensitive IPN hydrogel microbeads for targeted delivery.

**Keywords:** gum kondagogu, interpenetrating polymer network, pH responsive, microbeads, diclofenac sodium, anti-inflammatory activity

## INTRODUCTION

Stimulus-responsive drug delivery systems can be fabricated employing hydrogels – networks of cross-linked three-dimensional polymers. Importantly, stimulus-reactive hydrogels can exhibit spectacular variations in their network structure, swelling behavior, and permeability. Also, they offer good mechanical strength in the

presence of electric current, pH, mechanical strength, temperature, and light.<sup>1</sup> Such hydrogels have drawn a lot of interest as smart materials that find uses in drug delivery systems.<sup>2</sup> Thus, drug delivery systems prepared from stimulus-reactive hydrogels can deliver the necessary amount of incorporated drugs at the right time and a specific

site in the body.<sup>3</sup> Fortunately, it is possible to control the swelling or shrinking of pH-dependent hydrogels, using the ionization of the -COOH groups of the polymer. At higher pH levels, the -COOH groups withstand ionization; but at lower pH levels, they become protonated. Following ionization, the network contains more counterions and the osmotic pressure between the hydrogel's interior and exterior fluids varies. The hydrogel will swell, counteracting the rise in osmotic pressure.<sup>2,3</sup> Thus, the pH-responsive hydrogels can deliver the drugs to a particular part of the body.<sup>4</sup>

Recently, the development of natural polymer-based multiparticles, such as microbeads, microspheres, and microcapsules, has been an area of intensive investigation.<sup>5</sup> These multiparticles can simply move across the gastrointestinal tract, reach equally over a greater area of the gastrointestinal tract, prevent revelation to higher drug concentrations, and release drugs in a modified pattern.<sup>6</sup> Biodegradability, biocompatibility, higher patient tolerance, low cost, easy availability, edibility, and non-toxicity are all significant advantages of natural polymers over synthetic materials.<sup>2,7,8</sup> However, there are several disadvantages to the use of natural gums. They are susceptible to uncontrolled hydration, microbial contamination, viscosity variations during storage, and so on.<sup>2</sup> These constraints can be overcome by employing blending, the creation of interpenetrated polymer networks (IPN), and cross-linking. Interestingly, the IPNs are a mixture of more than one polymer in a network system, one of them is produced and/or crosslinked in the direct presence of another one.<sup>9</sup> The IPNs prepared utilizing natural polymers can distribute drugs at a steady rate across an extended period. Homopolymers on their own cannot meet up such challenging requirements concerning both properties and performance.<sup>10</sup> Also, IPNs have denser network structures that are responsible for superior mechanical properties and the level of crosslinking among the polymers determines the drug release behaviour.<sup>9,11</sup> Therefore, we intend to design pH-sensitive IPN hydrogel microbeads as a superior gastroprotective drug delivery system.

Currently, many natural polymers are being utilized for making IPNs. One such natural polymer that is yet to be explored is gum kondagogu (GK), an anionic polysaccharide tree exudate from *Cochlospermum gossypium* (family: Bixaceae).<sup>12,13</sup> It is widely available,

biocompatible, cost-effective, and biodegradable.<sup>14,15</sup> It has been used to design sponges for wound healing applications, gelling agents, emulsifying agents, *etc.*<sup>14</sup> Despite these applications, natural polysaccharides are suffering from plenty of demerits, mainly including lower shelf life, viscosity modification, solubility issue, and uncontrolled hydration, which limit their practical applications in the design of pharmaceutical dosage forms.<sup>16</sup> Hence, there is a desire to modify the GK using suitable agents to overcome such disadvantages.

Polyacrylamide (pAAm) is a widely used polymer for several applications due to its unique and versatile characteristics. One of them is that pAAm can hold a substantial portion of water inside its structure and swells once immersed in water. These attractive characteristics made pAAm appropriate for the delivery of drugs.<sup>11</sup> Therefore, we intend to use the pAAm as a grafting agent for GK to design pH-responsive pAAm-modified GK.

Sodium alginate (SA) is utilized as a gelling agent, comprising 1,4-linked- $\beta$ -D-mannuronic acid and  $\alpha$ -L-guluronic acid. It has the feature of undergoing gelation in the presence of cations. During ionic gelation, sodium ions are replaced by the cations from the surrounding environment. Mainly, a crosslinked alginate is valuable in the regulated release of drugs. Also, SA can be crosslinked covalently utilizing glutaraldehyde.<sup>17-20</sup> Therefore, SA is a good candidate for the design of IPN based drug delivery systems. To date, polyvinyl alcohol-SA,<sup>21</sup> poly(methacrylic acid)-SA,<sup>22</sup> locust bean gum-SA,<sup>23</sup> tamarind seed polysaccharide-SA,<sup>5</sup> and carrageenan-SA,<sup>24</sup> *etc.* have been used for the controlled release of loxoprofen, theophylline, capecitabine, diltiazem hydrochloride, and ketoprofen respectively. Consequently, we propose to design pH-responsive IPN hydrogels microbeads using hydrolyzed pAAm-GK and SA as a major constituents.

Diclofenac sodium (DS) functions as a non-steroidal anti-inflammatory drug (NSAID), displaying minimal solubility under acidic pH conditions, and becoming soluble within alkaline pH environments. The biological half-life of diclofenac sodium is 1-2 h.<sup>25</sup> It is being utilized in the long-lasting therapy of rheumatoid arthritis, ankylosing spondylitis, and osteoarthritis. It is mainly used for pain and fever. However, the frequent administration of DS produced various adverse effects, like hypersensitivity reactions,

ulceration or perforation of the intestinal wall, mild dyspepsia, depression of renal functions, bleeding, *etc.*<sup>26-28</sup> Consequently, the utilization of pH stimuli responsive IPN hydrogel microbeads composed of hydrolyzed (H)-pAAm-g-GK and SA could present a more advanced approach for delivering DS in a gastroprotective manner, a strategy that has not been previously documented.

Within this research endeavor, we elucidate the preparation of pH-responsive IPN-mediated hydrogel microbeads, employing H-pAAm-g-GK and SA as constituents, aimed at facilitating the gastroprotective conveyance of DS. In brief, pAAm was grafted onto the backbone of GK using microwave-assisted polymerization. Herein, the -CONH<sub>2</sub> groups of pAAm were then transformed into -COO groups via alkaline hydrolysis to produce a pH-sensitive polymer. Further, using the crosslinker glutaraldehyde, this hydrolyzed pAAm-g-GK was crosslinked with SA to generate a three-dimensional pH-sensitive IPN matrix that gives better drug entrapment efficiency. Also, the formulated IPN microbeads were spectroscopically characterized and then *in vitro-in vivo* parameters were assessed. Essentially, the formulated pH-sensitive IPN hydrogel microbeads containing carboxyl functional groups remain unionized in the acidic pH, resulting in a limited amount of DS release. Besides, it ionizes in the basic pH, resulting in a larger amount of DS release. The optimized pH-responsive IPN hydrogel microbeads exhibited significant anti-inflammatory activity in albino Wistar rats, validating the pH-triggered and sustained release of DS. Overall, the designed pH-stimuli responsive IPN-based hydrogel microbeads of H-pAAm-g-GK and SA can be used as an excellent carrier for the gastroprotective oral delivery of DS and other actives. In the future, it is necessary to develop an appropriate system, such as a capsule, for the oral administration of the designed pH-responsive IPN-based hydrogel microbeads.

## EXPERIMENTAL

### Materials

Diclofenac sodium (DS) was generously provided as a gift sample by Ajanta Pharmaceuticals, located in Mumbai, India. Gum kondagogu (Grade I) (GK) was obtained as a gift sample from Girijan Cooperative Corporation, Hyderabad, India. The following chemicals and reagents: sodium alginate (SA; low viscosity), acrylamide (AAm; 98% purity), ammonium persulfate (98% purity), glutaraldehyde (25% w/v),

sodium hydroxide (NaOH; 97% purity), methanol (99% purity), and calcium chloride (95% purity), were bought from Loba Chemie Pvt. Ltd. All analytical-grade chemicals and reagents employed in the formulation and analysis of pH-responsive IPN hydrogel microbeads were utilized as received, without undergoing any additional purification processes.

### Synthesis of H-pAAm-g-GK

In this study, the microwave-assisted synthesis of pAAm-g-GK was performed, with slight modifications of the method previously documented.<sup>29</sup> Firstly, GK (2%, w/v) was dissolved using double distilled water in 100 mL of a glass beaker via bath sonication for 2 h. Following this, the obtained dispersion was subjected to stirring at 1000 rpm for 24 h. After this step, 80 mL of the mixture was dissolved in a solution (100 mL) of polyacrylamide (10 mM) and ammonium persulfate (20 mM), followed by continuous stirring at 500 rpm for 1 h. Here, the obtained polymeric solution was placed in a microwave oven and irradiated at 900W for 1 min, wherein 3 cycles were performed. The temperature of the prepared polymer solution was evaluated by positioning a thermometer within the reaction container, revealing that it remained below 70 °C. After completion of this step, the final reaction mixture was subjected to cooling in ice-cold water. After grafting, the pAAm-g-GK was thoroughly rinsed with a mixture of distilled water and methanol (80:20) to ensure the effective removal of any unreacted monomers and by-products. The washing process is critical for reducing residual polyacrylamide, which was quantitatively assessed using UV spectroscopy. The purified pAAm-g-GK was subsequently dried at 40 °C to obtain the final product. The grafting efficiency (%) was estimated by employing Equation (1). Herein, W<sub>0</sub> represents the weight of GK, and W<sub>1</sub> represents the weight of the pAAm-g-GK. Also, W<sub>2</sub> represents the weight of acrylamide.<sup>16</sup>

$$\text{Grafting efficiency (\%)} = \frac{W_1 - W_0}{W_2} \times 100 \quad (1)$$

To achieve the hydrolysis of pAAm-g-GK, 1 g of pAAm-g-GK was stirred into a solution containing 50 mL of 0.9 M NaOH. In this process, the reaction was subsequently carried out at a temperature of 75 °C for a duration of 1 h, employing a temperature-regulated steam bath. After this step, the product was cooled down at room temperature, following which 200 mL of methanol was added. Finally, the obtained mixture was allowed to dewater for 12 h. Once the 12 h period was completed, the resulting H-pAAm-g-GK was isolated, subjected to three rounds of rinsing with methanol, and subsequently dried at 50 °C utilizing an oven.<sup>11</sup>

### Design of IPN-based microbeads

During this step, the pH-responsive IPN-mediated hydrogel microbeads were synthesized by incorporating H-pAAm-g-GK and SA. To outline the process briefly, a polymeric solution was created by

combining pAAm-g-GK and SA at a concentration of 4% w/v in double-distilled water. The solution was then subjected to continuous stirring at 500 rpm for a continuous duration of 4 h. After this, an accurate 20 mg of DS was added into the polymer solution and blended evenly using the stirring process at 100 rpm for 30 minutes. After completion of both processes, the obtained polymeric dispersion was then filled into a 20 mL hypodermal syringe and then it was gradually dropped into a CaCl<sub>2</sub> aqueous solution, followed by constant stirring at 100 rpm. In this context, the microbeads were retrieved from the CaCl<sub>2</sub> solution, and subsequently underwent a purification process involving two rounds of washing using 50 mL of distilled water each. After this purification step, the

microbeads were allowed to dry at a temperature of 40 °C for a duration of 12 h, following a 24 h period at room temperature. Finally, the obtained microbeads were commenced for covalent crosslinking in methanol containing various amounts of glutaraldehyde and 1N HCl at 50 °C for 30 min. Subsequently, in order to eliminate any residual unreacted glutaraldehyde, the dual cross-linked IPN microbeads were subjected to rinsing with distilled water. Following this rinsing process, the microbeads were dried at 40 °C overnight in a vacuum oven. Here, the absence of unreacted GA after washings by 2,4-dinitrophenyl hydrazine was demonstrated by a negative test.<sup>30</sup> The composition of different IPN microbeads is specified in Table 1.

Table 1  
Preparation of IPN microbeads for delivery of DS

Batch no.	H-pAAm-g-GK (%w/v)	SA (%w/v)	Diclofenac sodium (%w/w)	CaCl <sub>2</sub> (%w/v)	GA (% w/w)
F1	-	4	20	5	-
F2	0.5	3.5	20	5	4
F3	1	3.0	20	5	4
F4	1.5	2.5	20	5	4
F5	2	2	20	5	4
F6	1.5	2.5	20	5	8
F7	1.5	2.5	20	10	8

**Spectroscopical characterization**

Fourier-transform infrared spectroscopy (FT-IR) analysis was conducted employing an 8400S Shimadzu instrument, Japan. This analysis encompassed GK, pAAm-g-GK, H-pAAm-g-GK, DS, and DS-loaded IPN microbeads, spanning the spectral range of 500 to 4000 cm<sup>-1</sup>. Differential scanning calorimetry (DSC) was employed to analyze the thermograms of DS, acrylamide, pAAm-g-GK, H-pAAm-g-GK, and DS-loaded IPN microbeads. This analysis was conducted under nitrogen flow, subjecting the samples to a heating rate of 10 °C per minute within the temperature range of 40 °C to 250 °C. The diffractograms of GK, acrylamide, pAAm-g-GK, DS, and DS-loaded IPN microbeads were analyzed using a powder X-ray diffractometer (PXRD). The analysis was conducted within the diffraction angle range of 0° to 80° (2θ). For the examination of the morphology of GK and pAAm-g-GK, scanning electron microscopy (SEM) was employed. During this analysis, the samples were coated with a layer of gold, and subsequently positioned within the sample cuvette. Images of the samples were then captured using a 10 kV accelerating voltage. The size of an average of 100 individual microbeads from each batch was gauged utilizing a digital micrometer. The micrometer boasted a measurement precision of ± 0.001 mm.

**Percent drug entrapment efficiency (%DEE)**

To measure the %DEE, the formerly described method was used. To summarize, all batches of IPN

microbeads (totaling N = 3) were meticulously weighed at 100 mg each and subsequently immersed in 50 mL of phosphate buffer with a pH of 7.4. This immersion process took place at a temperature of 37 °C and lasted for a duration of 12 h. After 12 h, the microbeads were crushed, followed by heating at 40 °C for 1 h. Subsequently, the resulting solution underwent cold centrifugation at 5000 rpm for a duration of 30 min. Following centrifugation, the absorbance of the supernatant fluid was measured using an ultraviolet-visible (UV-Vis) spectrophotometer (UV-1800, Shimadzu, Japan), specifically at a wavelength of 276 nm.<sup>31</sup> Finally, the %DEE was quantified using Equation (2):

$$\% \text{ DEE} = \frac{\text{Pract. yield}}{\text{Theor. yield}} \times 100 \tag{2}$$

**Pulsatile swelling study**

Pulsatile swelling analysis was chosen as the preferred method to validate the dynamic pH-dependent swelling and shrinking nature of the prepared pH-sensitive IPN microbeads. In brief, 20 mg of IPN microbeads (N=3) precisely were added to 25 mL of buffer solution of pH of 7.4 and 1.2, separately at 37 °C. After a specified time interval, the IPN microbeads were retrieved from the buffer solution, and any surface-adhered droplets were eliminated using tissue paper. The weight of the IPN microbeads was then measured using an electronic microbalance. The percentage swelling (Q) was calculated using

Equation (3), where  $W_1$  signifies the mass of the dry IPN-based prepared microbeads, and  $W_2$  represents the mass of the soaked IPN microbeads.<sup>32</sup>

$$Q = \frac{W_2 - W_1}{W_1} \times 100 \quad (3)$$

#### ***In vitro* dissolution study of prepared DS-loaded IPN hydrogel microbeads**

For the *in vitro* dissolution analysis of the prepared DS-loaded microbeads, a basket-type dissolution apparatus I (EDT.08LX, Electro Lab, India) was employed. The procedure began by adding a precise mass of IPN microbeads ( $F_1$ ,  $N = 3$ ) to two separate dissolution media: one with a pH of 1.2 and another with a pH of 7.4, totaling 900 mL each. The dissolution process was conducted at a programmed temperature of  $37 \pm 0.5$  °C, while the paddle rotation was set to 50 rpm. For the quantification of DS release concentration in the dissolution media, 5 mL aliquots were collected at various time intervals. In order to uphold the sink condition, a matching volume of the corresponding buffer solution was introduced after each collection. In this step, the collected samples were purified using a  $0.45 \mu\text{m}$  membrane filter. Finally, samples were scanned using a UV-visible spectrophotometer (UV-1800, Shimadzu, Japan), operating at a wavelength of 276 nm to determine the drug concentration release into both buffers (pH 1.2 and pH 7.4). The same process was repeated for all batches ( $F_2$ - $F_7$ ) to ensure the DS release from prepared microbeads.

#### ***In vivo* anti-inflammatory activity**

In order to validate the *in vivo* anti-inflammatory activity of the formulated DS-loaded microbeads, adult albino Wistar rats, approximately 8 weeks old, were utilized. The study was conducted in accordance with ethical guidelines and was approved by the Institutional Animal Ethics Committee with reference number IAEC/RCPIPER/2021-22/31. The animal study complied with the guidelines provided by the committee for the purpose of control and supervision of experiments on animals (CPCSEA), Government of India. Importantly, the animal experiments performed in this research work comply with the ARRIVE guidelines and were carried out in accordance with the U.K. Animals (Scientific Procedures) Act of 1986 and its associated guidelines. In short, albino Wistar rats ( $200 \pm 20$  g) were parted into three groups, wherein Group I, Group II, and Group III represent the control group ( $N = 6$ ), standard group ( $N = 6$ ), and the test group ( $N = 6$ ), respectively. Following a method previously described in the literature, the carrageenan-induced paw edema procedure was utilized to evaluate the *in vivo* anti-inflammatory action.<sup>33</sup> The swelling was induced using 0.1 mL of 1% w/v carrageenan solution into the rat's left hind paw of the sub-plantar region. Then, 1 mL of 0.5% w/v NaCMC solution was administered orally to the rats in the control group.

Similarly, the rats in the standard group received 10 mg/kg of pure DS. In the case of the test group, DS-loaded IPN microbeads ( $F_4$ ) were preferred wherein the concentration of DS was considered similar to group II concentration.<sup>34</sup> Oral administration was carried out using a solution of NaCMC (0.5% w/v), along with pure DS and DS-loaded IPN microbeads  $F_4$ . After 30 min of incorporation of pure diclofenac sodium and DS-loaded IPN microbeads  $F_4$ , the carrageenan was injected into each rat from the control and test groups. Lastly, the percentage of paw edema inhibition and the paw volume of rats were measured using a plethysmometer.<sup>31</sup>

## **RESULTS AND DISCUSSION**

The pAAm-g-GK polymer was synthesized via a microwave-assisted technique, wherein GK (natural polysaccharide) was grafted using pAAm. Here, GK contains pendant O-H groups, whereas microwave irradiation produces dielectric heating of GK particles, and ensures the breakage of O-H links, leading to GK macromolecules. The persulfate free radicals can also produce these macroradicals by absorbing hydrogen ions.<sup>35</sup> The free radicals then combine with acrylamide, initiating a chain reaction that leads to the creation of graft polymer (pAAm-g-GK). The residual acrylamide concentration in the pAAm-g-GK sample after washing was quantified as 0.02 mg/g, indicating an effective removal process. This low residual content is within acceptable safety limits, ensuring the biocompatibility of the final product. To transfer the hydrolysis of the generated graft polymer (H-pAAm-g-GK) into the pH-sensitive carrier, standard sodium hydroxide was used, wherein pAAm's  $-\text{CONH}_2$  groups are converted to  $-\text{COONa}$  ions by alkaline hydrolysis, yielding a pH-sensitive polymer.<sup>16</sup>

#### **FT-IR spectroscopy**

Figure 1 displays the FT-IR spectra of different samples: GK (a), pAAm-g-GK (b), H-pAAm-g-GK (c), DS (d), and DS-loaded IPN microbeads  $F_4$  (e). In the FT-IR spectrum of GK (Fig. 1A), distinctive absorption peaks at  $3450.15 \text{ cm}^{-1}$ ,  $1680.01 \text{ cm}^{-1}$ , and  $1420.05 \text{ cm}^{-1}$  can be attributed to the  $-\text{O}-\text{H}$  stretching,  $-\text{CH}_3-\text{CO}$  group, and  $-\text{COO}-$  group of uronic acid residue, respectively.<sup>12</sup> In the FT-IR spectrum of pAAm-g-GK, an absorption band at  $3450.77 \text{ cm}^{-1}$  was observed, indicating the merging of  $-\text{O}-\text{H}$  stretching from the hydroxyl groups of GK and N-H stretching of amides (as shown in Fig. 1B). The presence of bands around  $1607.72 \text{ cm}^{-1}$  and  $1431.23 \text{ cm}^{-1}$  confirmed the existence of the

primary amide group on GK, thereby confirming the occurrence of the grafting reaction.<sup>16</sup> In the FT-IR spectrum of H-pAAm-g-GK, distinct bands were observed at 3447.87  $\text{cm}^{-1}$ , 2923.22  $\text{cm}^{-1}$ , and 1611.58  $\text{cm}^{-1}$ , corresponding to -O-H stretching vibrations, -C-H stretching vibrations, and -COO-stretching groups vibrations, in that order (as depicted in Fig. 1C). The band at 1039  $\text{cm}^{-1}$  present in pAAm-g-GK was absent in H-pAAm-g-GK, indicating the absence of the -NH band. This FT-IR analysis confirmed the hydrolysis of pAAm-g-GK.<sup>31</sup> The FT-IR spectrum of DS (as shown in Fig. 1D) displayed notable absorption bands at specific wavenumbers: 1405  $\text{cm}^{-1}$ , 1556

$\text{cm}^{-1}$ , 1574  $\text{cm}^{-1}$ , 3386  $\text{cm}^{-1}$ , and 746  $\text{cm}^{-1}$ . These corresponded to distinct vibrational modes, specifically -C-N stretching vibrations, -C=C-stretching vibrations, -C=O stretching vibrations, -N-H stretching vibrations, and -C-Cl stretching vibrations, respectively.<sup>36</sup> In the FT-IR of DS-loaded H-pAAm-g-GK@SA IPN microbeads (F4), as depicted in Figure 1E, a distinct peak at 1741  $\text{cm}^{-1}$  was observed, attributed to the -C=O group. Another peak at 3386  $\text{cm}^{-1}$ , specific to DS, indicated compatibility between the polymer and DS. This confirmed the successful incorporation of DS within the microbeads.

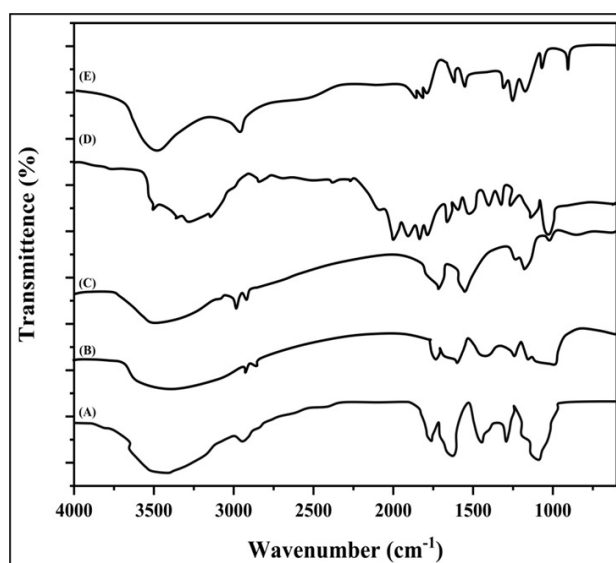


Figure 1: FT-IR spectra of (A) GK, (B) pAAm-g-GK, (C) H-pAAm-g-GK, (D) DS, and (E) optimized batch (DS-loaded H-pAAm-g-GK@SA IPN hydrogel microbeads-F4)

### SEM and elemental analysis

Figure 2A and B shows the surface morphology of GK, whereas Figure 2C and D shows the SEM images of pAAm-g-GK. The results indicate that grafting acrylamide onto GK led to a transformation in the shape and surface morphology of GK. However, it is noteworthy that the surface of pAAm-g-GK exhibits a higher density of grooves, compared to the rough surface of the original GK.<sup>16</sup> On account of H-pAAm-g-GK, the surface morphology is more spongy than that of pAAm-g-GK, with fewer grooves on the surface (Fig. 2E and F). Figures 2G and 2H depict the spherical morphology of DS-loaded H-pAAm-g-GK@SA IPN hydrogel microbeads-F4, characterized by a porous polymeric network. In summary, the SEM images corroborate the successful preparation of DS-loaded H-pAAm-g-

GK@SA IPN hydrogel microbeads-F4, utilizing the synthesized H-pAAm-g-GK as a foundation. The elemental composition analysis of GK revealed the presence of 0.22 wt% nitrogen, 34.97 wt% carbon, and 5.58 wt% hydrogen. These findings suggest the existence of minor protein traces within the GK structure. Besides, the pAAm-g-GK shows 12.41 wt% of nitrogen, 40.41 wt% of carbon, and 8.59 wt% of hydrogen. This could be related to the CONH<sub>2</sub> group of pAAm that occurs on the backbone of GK. Similarly, the hydrolyzed pAAm-g-GK had a lower nitrogen concentration (4.01 wt%), which may be because of the alteration of CONH<sub>2</sub> groups into COONa groups via alkaline hydrolysis. As a result, the reactions of grafting and alkaline hydrolysis were approved using elemental analysis.



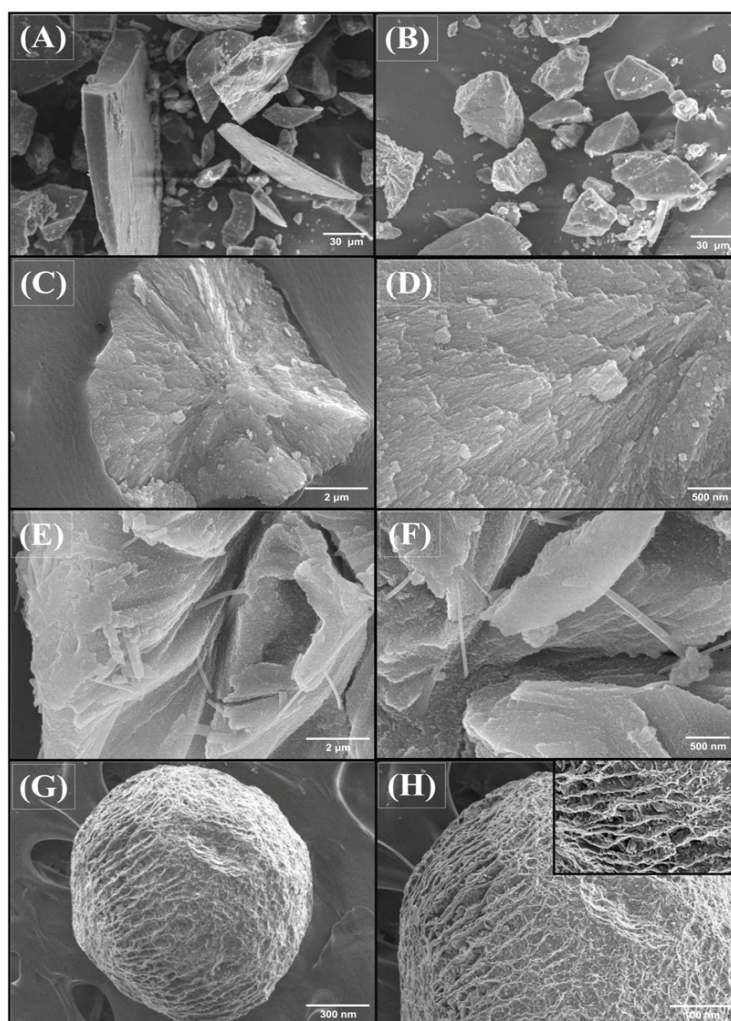


Figure 2: SEM images of GK (A, B), pAAM-g-GK (C, D), H-pAAM-g-GK (E, F), DS loaded H-pAAM-g-GK@SA IPN hydrogel microbeads-F4 (G, H)

### DSC analysis

Figure 3 displays the thermograms of GK (A), acrylamide (B), pAAM-g-GK (C), H-pAAM-g-GK (D), DS (E), and DS-loaded H-pAAM-g-GK@SA IPN hydrogel microbeads F4. In brief, Figure 3A shows the thermogram of GK. It shows the broad endotherm at 104.5 °C, which confirms the amorphous nature of GK. The thermogram of acrylamide shows a prominent endothermic peak at 85.48 °C (Fig. 3B),<sup>16</sup> confirming the crystalline nature. In Figure 3C, the thermogram of pAAM-g-GK reveals two distinct endothermic peaks at 178 °C and 230 °C. In this case, shifting of the endothermic peak towards high temperature supports the grafting reaction on the surface of GK. In Figure 3D, the thermogram of H-pAAM-g-GK exhibits a notable endothermic peak at 174 °C, which can be attributed to a modification in the thermal characteristics of pAAM-g-GK. This

is because of the transformation of the amide group into the carboxylic group. An additional peak was observed at 254 °C, indicating the formation of hydrogen bonds between the amine group from the surface functionality of pAAM-g-GK and the carboxylic (COOH) functionality from H-pAAM-g-GK.<sup>37</sup> The thermogram of DS is illustrated in Figure 3E, displaying an endothermic peak at 284.74 °C, which affirms the existence of crystallinity.<sup>38</sup> Finally, the thermogram of DS-loaded H-pAAM-g-GK@SA IPN hydrogel microbeads (F4) shows the two endothermic peaks at 173 °C and 284 °C (Fig. 3F). The reduction in the peak intensity of DS within DS-loaded H-pAAM-g-GK@SA IPN hydrogel microbeads signifies the conversion from a crystalline state to an amorphous state. This observation strongly suggests the successful

incorporation of DS into the proposed DS-loaded H-pAAm-g-GK@SA IPN hydrogel microbeads.

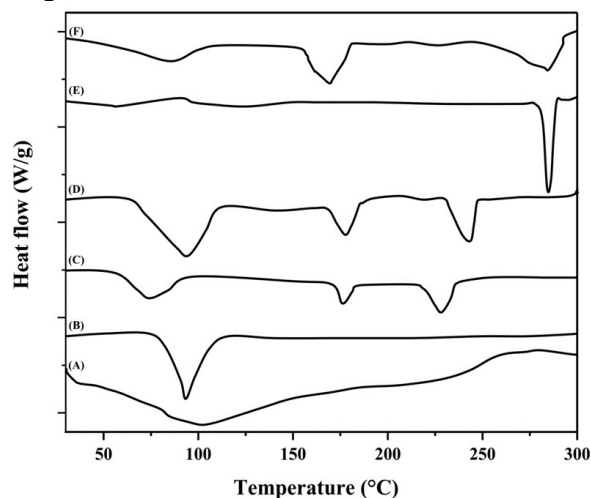


Figure 3: Thermograms of (A) GK, (B) polyacrylamide, (C) pAAm-g-GK, (D) H-pAAm-g-GK, (E) DS, (F) DS-loaded H-pAAm-g-GK@SA IPN hydrogel microbeads-F4

### PXRD analysis

Figure 4 displays diffractograms of various substances, including GK (A), acrylamide (B), pAAm-g-GK (C), H-pAAm-g-GK (D), DS (E), and DS-loaded H-pAAm-g-GK@SA IPN hydrogel microbeads F4 (F). The diffractogram of GK showed the absence of an intense peak in the range of 5 to 80° that confirmed the amorphous state of GK (Fig. 4A). The diffractogram of acrylamide displays the characteristic peaks at 12.49°, 19.70°, 24.12°, and 28.96°, indicating the crystalline nature of acrylamide (Fig. 4B). The diffractogram of pAAm-g-GK is displayed in Figure 4C. In this diffractogram, the characteristic peaks of acrylamide at 14.82°, 20.12°, 25.72°, and 29.72° may be seen, but with decreased peak intensity, which may be because of grafting of pAAm on GK and the formation of pAAm-g-GK.<sup>16</sup> The diffractogram of H-pAAm-g-GK (Fig. 4D) displays the change in the diffraction pattern of H-pAAm-g-GK, which may be because of the hydrolysis process on H-pAAm-g-GK. The diffractogram of DS (Fig. 4E) exhibited a highly intense peak in the range of 5° to 25° (2θ), showing a crystalline form of DS. Figure 4F shows the diffractogram of DS-loaded H-pAAm-g-GK@SA IPN hydrogel microbeads (F4), wherein the peak intensity of DS was found to be reduced, compared to the peak intensity obtained in the diffractogram of DS. Importantly, it assured the incorporation followed by molecular level dispersion of DS into H-pAAm-g-GK@SA IPN hydrogel microbeads.<sup>36</sup>

### Particle size analysis

In the case of the development of IPN microbeads, the prepared polymeric dispersion was added into the counter ion solution, wherein the ionic crosslinking happened amongst SA containing two strands. In this process, calcium ions ( $\text{Ca}^{2+}$ ) undergo exchange with sodium ions ( $\text{Na}^{+}$ ) from the SA molecules at the  $\text{COO}^-$  groups during ionic crosslinking. Additionally, another SA chain gets links with a  $\text{Ca}^{2+}$  ion, forming a bond. Consequently, the  $\text{Ca}^{2+}$  ions connect with two SA chains, leading to the creation of a spherical matrix that encapsulates both the uncrosslinked pAAm-g-GK and DS components. Importantly, after drying the microbeads, such ionically crosslinked IPN microbeads lose their shape and look like flat discs. This could be because of the beads' lesser mechanical power. Therefore, ionically crosslinked microbeads dipped in GA resulted in an acetal structure. It is created by the interaction of the -OH groups of SA and pAAm-g-GK with the -CHO groups of GA. It ensues in an IPN composed of SA and pAAm-g-GK.<sup>36</sup> During this stage, the IPN beads exhibited a spherical shape with surface grooves. This phenomenon can be attributed to heightened particle mechanical forces and the involvement of SA in the manufacturing process. Consequently, the size of the IPN microbeads fell within the range of  $689.65 \pm 1.25$  to  $727.77 \pm 1.73 \mu\text{m}$ , as indicated in Table 2. Notably, the size of these microbeads demonstrated a direct correlation with the quantity of pAAm-g-GK present. Herein, the hydrodynamic viscosity assumption states that an



increase in pAAm-g-GK amount results in an increase in the polymeric solution's thickness, causing bigger droplets to be formed during the ejection through the needle, ensuing in larger microbeads.<sup>39</sup> On the contrary, an elevation in the  $\text{Ca}^{2+}$  concentration led to a decrease in the microbeads' size. It is important to highlight that, even after subjecting the ionically crosslinked

microbeads to glutaraldehyde treatment, their size still decreased. At high crosslink density, the polymer matrix shrinks rapidly during crosslinking, resulting in smaller and stiffer IPN.<sup>40,41</sup> Here, the average particle size of the optimized batch (F4) was found to be  $725.10 \pm 1.11 \mu\text{m}$ .

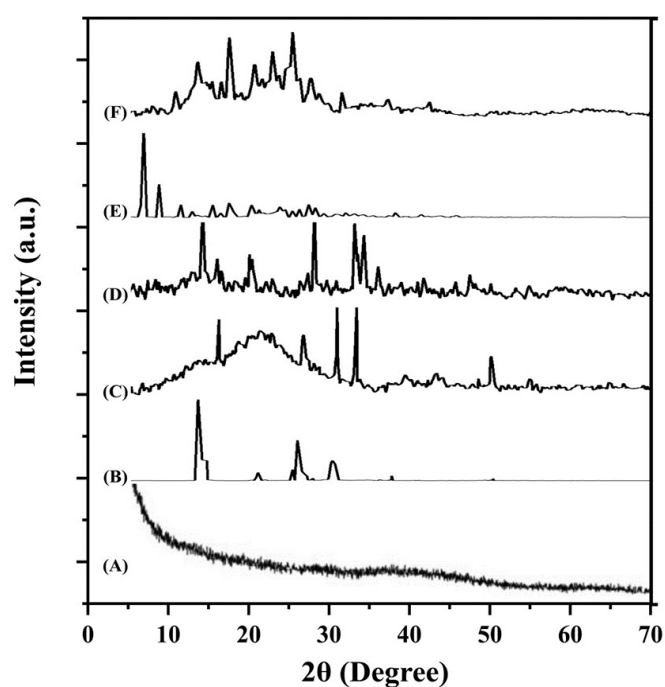


Figure 4: Diffractograms of (A) GK, (B) polyacrylamide, (C) pAAm-g-GK, (D) DS, (E) DS-loaded H-pAAm-g-GK@SA IPN hydrogel microbeads-F4

Table 2  
Particle size and DEE of all batches

Sr. No.	Batch code	Particle size ( $\mu\text{m}$ )	DEE (%)
1	F1	$692.45 \pm 1.22$	$79.35 \pm 0.65$
2	F2	$689.65 \pm 1.25$	$87.23 \pm 0.54$
3	F3	$718.53 \pm 1.23$	$89.65 \pm 0.15$
4	F4	$725.10 \pm 1.11$	$92.45 \pm 0.12$
5	F5	$727.77 \pm 1.73$	$88.57 \pm 0.48$
6	F6	$715.25 \pm 1.26$	$86.85 \pm 0.43$
7	F7	$710.65 \pm 1.65$	$82.71 \pm 0.79$

N= 100;  $\pm$ : Standard deviation

### %DEE

The %DEE of DS in the obtained IPN microbeads was found to be within  $79.35 \pm 0.65\%$  to  $92.45 \pm 0.12\%$  (Table 2). Within these IPN microbeads, an augmentation in the quantity of H-pAAm-g-GK leads to a significant enhancement in the %DEE. Similarly, the rise in pAAm-g-GK or SA proportion resulted in a slightly increased %DEE. In this research work, the pAAm-g-

GK/SA beads demonstrate a higher %DEE value than pure SA beads. Importantly, as more pAAm-g-GK is present in the system, the polymer content and viscosity of the polymer solution are increased. As an outcome, the polymer captures more molecules of DS, enhancing the effectiveness of entrapment efficiency.<sup>42</sup> The DEE of IPN microbeads formulated by a smaller concentration of  $\text{Ca}^{+2}$  ions was found to be less.

Possibly, it is because of insufficient crosslinking. Due to this, the matrix may become saggy and DS loss may occur from the IPN matrix during microbead preparation. When IPN microbeads were produced using a higher concentration of  $\text{Ca}^{2+}$  ions, the IPN matrix exhibited increased rigidity. Simultaneously, the loss of DS was diminished, leading to a higher DEE.<sup>31</sup> In the case of the GA effect on the DEE of beads, DEE was found to be greatly reduced as the amount of GA was increased. This might be attributed to enhanced stiffness and decreased free volume present inside the matrix. More GA solution (4 to 8% w/w GA, respectively) dissolved inside the beads, enabling the DS to disintegrate and disperse in the microbeads. Consequently, this led to a reduction in the %DEE for DS in the prepared IPN microbeads.<sup>11</sup>

### Pulsatile swelling analysis

As per the literature, the swelling behavior of the polymer controls the release of active agents from a polymeric matrix. In this work, the swelling investigation of the proposed systems was conducted at a phosphate buffer of pH 7.4 and a buffer solution of pH 1.2. As an outcome, it may aid to describe the DS release behavior of the IPN-based microbeads. Figure 5A shows the pH-sensitive swelling behavior of all prepared batches – F1 to F7. In summary, the microbeads created with SA (F1) displayed relatively low sensitivity to changes in pH. In contrast, the IPN microbeads fabricated using pAAM-g-GK and SA exhibited a more pronounced response to pH variations. Here, Figure 5A confirmed that altering the pH of the surrounding environment between pH 1.2 to pH 7.4 caused a significant rise in swelling in all of the beads. Possibly, because the COO- groups of the beads stay protonated in acidic solutions and produces a negligible electrostatic force of attraction, the beads swell to a lesser level.<sup>43</sup> However, at greater pH 7.4, the COO- groups of the beads endure ionization, and the osmotic pressure within the beads rises, ensuing in more swelling. In addition, it can be influenced by the polymer concentration and extent of cross-linking of the beads. Swelling is enhanced by increasing the amount of H-pAAM-g-GK in the microbeads. The polymeric network is weak, as well as a larger hydrodynamic free volume at low polymer concentrations, allowing more buffer solution to be absorbed and resulting in more swelling.<sup>2</sup> Moreover, it was discovered that as the amount of GA increased, the swelling

of the microbeads decreased. The rising GA concentration to 8% resulted in lower swelling in both acidic and alkaline media. It might be owing to the establishment of a firm rigid network structure at high cross-link densities.<sup>44</sup> Overall, it assured the pH-responsive behavior of DS microbeads.

### *In-vitro* dissolution analysis

Figure 5B illustrates the *in vitro* dissolution profile of DS from the prepared IPN-based microbeads. In summary, the hydrogel microbeads containing SA exhibited rapid DS release, achieving approximately complete release within 6 h, when exposed to a dissolution medium with a pH of 7.4. Conversely, when subjected to a dissolution medium with a pH of 1.2, these microbeads exhibited around 50% DS release within 2 h. On the other hand, the IPN hydrogel microbeads created from H-pAAM-g-GK and SA showcased pH-sensitive DS release characteristics. This behavior could be attributed to the presence of a higher concentration of carboxyl functional groups in H-pAAM-g-GK and the enhanced mechanical strength resulting from the IPN design.<sup>24</sup> Nonetheless, the IPN hydrogel microbeads based on H-pAAM-g-GK exhibit a more substantial release of DS under pH 7.4 conditions, while demonstrating reduced DS release in pH 1.2 dissolution media over a 12-h period. This phenomenon can be attributed to the heightened swelling behavior of H-pAAM-g-GK-based IPN hydrogel microbeads in a buffer with a pH of 7.4. The COO- functional groups within the IPN beads undergo ionization at higher pH levels, leading to an increase in the osmotic pressure within the beads. This elevated osmotic pressure results in more pronounced swelling and, consequently, a faster DS release from the prepared IPN hydrogel microbeads. On the contrary, in an acidic pH of 1.2, the electrostatic repelling force diminishes as the COO- groups transition to an unionized form. This shift is thermodynamically favorable for this pH range. Consequently, the beads experience reduced swelling and, in turn, exhibit lower DS release.<sup>45</sup> Furthermore, it was evident that the release of DS from the prepared IPN hydrogel microbeads was significantly influenced by the quantities of pAAM-g-GK and crosslinkers employed. Notably, the DS release from IPN microbeads (labeled as F6-F7) exhibited a decrease with increasing  $\text{Ca}^{+2}$  ion concentration. This effect can primarily be attributed to the reduction in the

available free volume within the matrix due to cross-linking. As a result, the release of DS is hindered. In contrast, the DS release from IPN microbeads (labeled as F2-F4) was observed to increase with higher amounts of H-pAAm-g-GK. Essentially, the incorporation of more H-pAAm-g-GK led to enhanced swelling of the IPN microbeads. This can be attributed to the hydrophilic nature of H-pAAm-g-GK, which facilitates the ingress of buffer molecules into the loaded IPN hydrogel microbeads. Consequently, this increased swelling encourages a greater amount of DS to be released from the microbeads.<sup>11</sup> Finally, various release kinetic

models, including zero order, Hixson Crowell, and Korsmeyer Peppas, were employed to validate the release pattern of DS from the prepared IPN-based hydrogel microbeads. The correlation coefficient ( $R^2$ ) for each batch (labeled as F1-F7) has been outlined in Table 3. The results indicate that the Korsmeyer Peppas model yields the best fit for all batches of microbeads. This suggests that the release of DS from the microbeads follows a mechanism described by the Korsmeyer Peppas model ( $R^2 = 0.9964$ ), reinforcing its applicability as the most accurate model for describing the release behavior across all tested batches.

Table 3  
Release kinetic analysis of pH-sensitive IPN for all batches (F1 to F7)

Batch No.	Zero-order ( $R^2$ )	Hixson-Crowell ( $R^2$ )	Korsmeyer-Peppas ( $R^2$ )
F1	0.7927	0.7657	0.8922
F2	0.9801	0.9488	0.9897
F3	0.9830	0.9478	0.9869
F4	0.9920	0.9715	0.9964
F5	0.9968	0.9702	0.9976
F6	0.9965	0.9773	0.9980
F7	0.9913	0.9619	0.9917

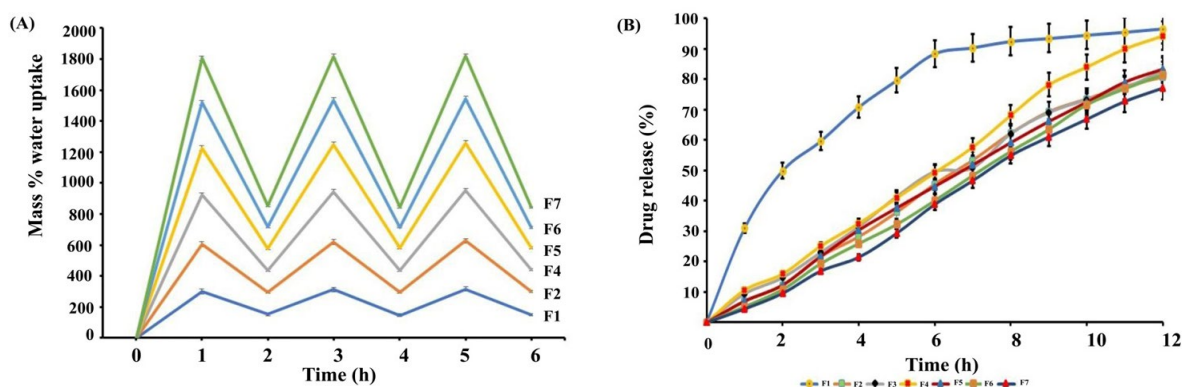


Figure 5: (A) Pulsatile swelling study of IPNs microbeads of batch F1 to F7; (B) *In vitro* release of DS from IPN microbeads of all batches in pH 1.2 (up to initial 2 h) and pH 7.4 dissolution media (from 2 h to 12 h)

### ***In vivo* anti-inflammatory activity**

In this research study, the results of the anti-inflammatory activity are presented in Figure 6. The control group initially showed a substantial 85.33% reduction in paw edema within 3 h, with a continued reduction of 17.21% after 12 h. When using the pH stimuli responsive DS-loaded H-pAAm-g-GK@SA IPN mediated hydrogel microbeads (labeled as F4), the edema inhibition percentage was lower at the start, measuring 27.28% within 3 h. The observed phenomenon of slow DS release from the pH-sensitive DS-loaded

H-pAAm-g-GK@SA IPN hydrogel microbeads (F4) in pH 1.2 buffer could likely be attributed to specific factors. In essence, the COOH functional groups present in the IPN beads remain uncharged at a pH of 1.2. Consequently, the osmotic pressure within the DS-loaded H-pAAm-g-GK@SA IPN hydrogel microbeads is not sufficiently elevated. This leads to limited swelling of the microbeads and subsequently results in the gradual release of DS from the prepared hydrogel microbeads. This inhibition gradually increased, reaching 83.83% after 7 h. Indeed, the observed phenomenon could

likely be attributed to the pH-sensitive nature of the DS-loaded H-pAAM-g-GK@SA IPN hydrogel microbeads (F4). In brief, the COO-functional groups within the IPN beads undergo ionization at a pH of 7.4. As a result of this ionization, the osmotic pressure within the DS-loaded H-pAAM-g-GK@SA IPN hydrogel microbeads increases significantly. This elevation in osmotic pressure leads to a greater degree of swelling in the microbeads. Consequently, this increased swelling contributes to a more rapid release of DS from the prepared hydrogel microbeads. This pH-responsive behavior showcases the designed microbeads' ability to release the drug in a controlled and efficient manner in response to changes in environmental pH. This behavior could be attributed to the presence of a higher concentration of carboxyl

functional groups in H-pAAM-g-GK. Finally, the % paw edema inhibition slightly dropped to 18.66% at the 12 h mark. Overall, the designed pH stimuli responsive DS-loaded H-pAAM-g-GK@SA IPN mediated hydrogel microbeads (F4) were formulated to exhibit enhanced drug release specifically in the intestinal (basic) environment, while minimizing release in an acidic environment. Also, a statistically significant difference (with a p-value < 0.05) was observed in the percentage inhibition of paw edema between the test group (F4) and both the control group and the standard group. This indicates that the pH-sensitive microbeads effectively controlled the release of the drug in a pH-responsive manner, contributing to their potential anti-inflammatory activity.

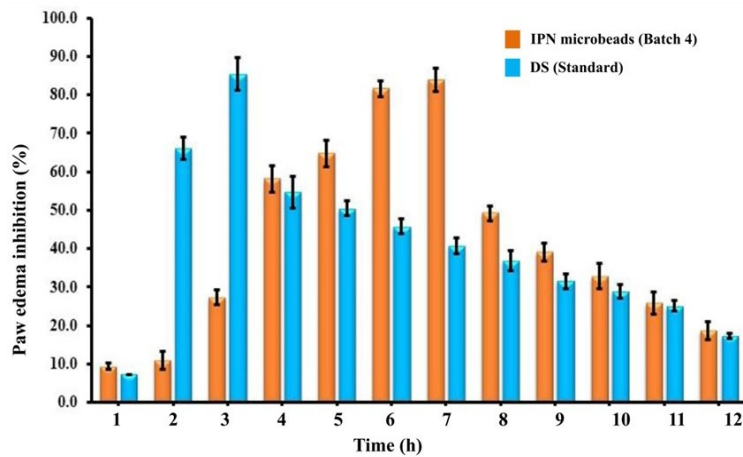


Figure 6: Assessment of anti-inflammatory activity performed on albino Wistar rats for pure DS (standard) and pH-sensitive DS-loaded H-pAAM-g-GK@SA IPN hydrogel microbeads (optimized batch: F4)

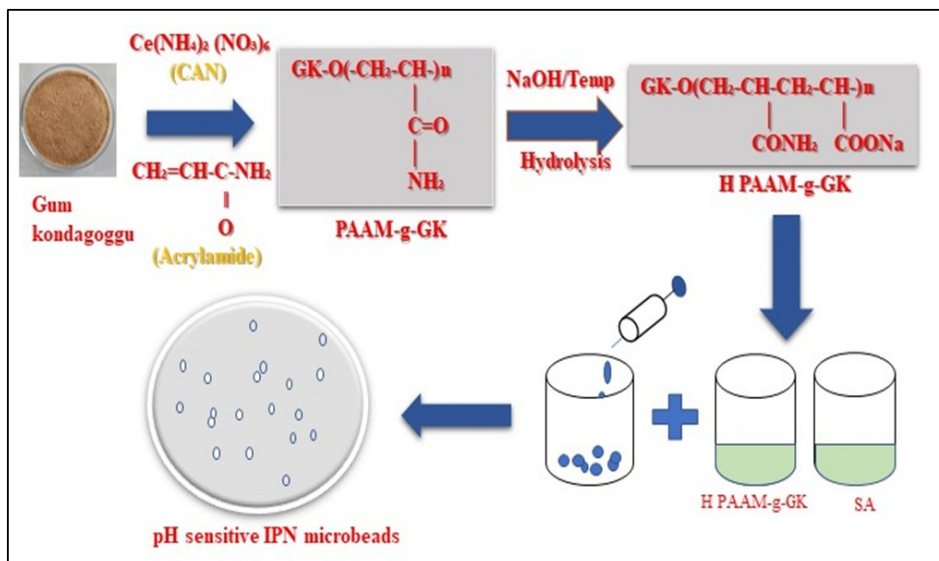


Figure 7: Polyacrylamide grafting of gum kondagogu

## CONCLUSION

In this research endeavor, pH-sensitive DS-loaded H-pAAM-g-GK@SA-based IPN hydrogel microbeads were fabricated through dual crosslinking for regulated oral delivery of DS with gastro-protective properties. To summarize, thermograms and diffractograms affirmed uniform molecular dispersion of DS within the IPN structure. In addition, the microbeads show spherical shape with a folded surface due to the dual crosslinking method forming the IPN with SA and H-pAAM-g-GK. Pulsatile swelling analysis indicated a pH-dependent increase in swelling, particularly at higher pH levels, where the COO- functional group ionized, boosting osmotic pressure within the IPN hydrogel microbeads. This led to heightened swelling at pH 7.4, facilitating increased DS release from pH-sensitive DS-loaded H-pAAM-g-GK@SA-based IPN hydrogel microbeads in buffer pH 7.4 dissolution media compared to buffer pH 1.2. In addition, *in vivo* anti-inflammatory activity demonstrated pH-responsive DS release from the hydrogel microbeads in both the stomach and intestine. As a result, the edema inhibition percentage was initially lower at 27.28% (3 h). However, it gradually increased to 83.83% by the end of 7 h. In conclusion, the designed pH-sensitive DS-loaded H-pAAM-g-GK@SA-based IPN hydrogel microbeads present an innovative approach for gastroprotective DS delivery. This research suggests the potential use of pH-sensitive natural polysaccharide-based H-pAAM-g-GK@SA-based IPN hydrogel microbeads to finely tune drug release in different pH environments, paving the way for enhanced drug delivery strategies in the future.

**ACKNOWLEDGMENT:** The authors extend their gratitude to the Management and Principal of the H. R. Patel Institute of Pharmaceutical Education and Research for providing the necessary facilities for the successful completion of this research. Mr. Sopan Nangare, one of the authors, would like to acknowledge the Indian Council of Medical Research (ICMR) in New Delhi for granting a Research Associate (RA) fellowship.

## REFERENCES

<sup>1</sup> R. Kulkarni and S. Biswanath, *J. Appl. Biomater. Biomech.*, **5**, 125 (2007), <https://doi.org/10.1177/22808000700500301>

- <sup>2</sup> R. V. Kulkarni and B. Sa, *Drug Dev. Ind. Pharm.*, **34**, 1406 (2008), <https://doi.org/10.1080/03639040802130079>
- <sup>3</sup> R. K. Drummond, J. Klier, J. A. Alameda and N. A. Peppas, *Macromolecules*, **22**, 3816 (1989), <https://doi.org/10.1021/ma00199a059>
- <sup>4</sup> O. Şanlı, N. Ay and N. Işıklan, *Eur. J. Pharm. Biopharm.*, **65**, 204 (2007), <https://doi.org/10.1016/j.ejpb.2006.08.004>
- <sup>5</sup> R. V. Kulkarni, S. Mutalik, B. S. Mangond and U. Y. Nayak, *J. Pharm. Pharmacol.*, **64**, 530 (2012), <https://doi.org/10.1111/j.2042-7158.2011.01433.x>
- <sup>6</sup> A. Halder and B. Sa, *AAPS PharmSciTech.*, **7**, E105 (2006), <https://doi.org/10.1208/pt070246>
- <sup>7</sup> P. Matricardi, C. D. Meo, T. Coviello, W. E. Hennink and F. Alhaique, *Adv. Drug Deliv. Rev.*, **65**, 1172 (2013), <https://doi.org/10.1016/j.addr.2013.04.002>
- <sup>8</sup> S. Maiti, M. Chowdhary, R. Datta, S. Ray and B. Sa, *J. Drug Target.*, **21**, 265 (2013), <https://doi.org/10.3109/1061186X.2012.745548>
- <sup>9</sup> T.-T. Hsieh, G. P. Simon and C. Tiu, *Polymer*, **40**, 3153 (1999), [https://doi.org/10.1016/S0032-3861\(98\)00204-3](https://doi.org/10.1016/S0032-3861(98)00204-3)
- <sup>10</sup> M. Changez, K. Burugapalli, V. Koul and V. Choudhary, *Biomaterials*, **24**, 527 (2003), [https://doi.org/10.1016/S0142-9612\(02\)00364-2](https://doi.org/10.1016/S0142-9612(02)00364-2)
- <sup>11</sup> R. V. Kulkarni and B. Sa, *Curr. Drug Deliv.*, **5**, 256 (2008), <https://doi.org/10.2174/156720108785915014>
- <sup>12</sup> V. Vinod, R. B. Sashidhar, K. I. Suresh, B. R. Rao, U. V. R. V. Saradhi *et al.*, *Food Hydrocoll.*, **22**, 899 (2008), <https://doi.org/10.1016/j.foodhyd.2007.05.006>
- <sup>13</sup> B. Janaki and R. Sashidhar, *Food Chem.*, **61**, 231 (1998), [https://doi.org/10.1016/S0308-8146\(97\)00089-7](https://doi.org/10.1016/S0308-8146(97)00089-7)
- <sup>14</sup> H. S. Rathore, M. Sarubala, G. Ramanathan, S. Singaravelu, M. D. Raja *et al.*, *Mater. Lett.*, **177**, 108 (2016), <https://doi.org/10.1016/j.matlet.2016.04.185>
- <sup>15</sup> H. S. Rathore, U. T. Sivagnanam, L. S. Abraham, D. Prakash, R. C. Panda *et al.*, *Polym. Bull.*, **79**, 7215 (2022), <https://doi.org/10.1007/s00289-021-03832-5>
- <sup>16</sup> S. Malik and M. Ahuja, *Carbohyd. Polym.*, **86**, 177 (2011), <https://doi.org/10.1016/j.carbpol.2011.04.027>
- <sup>17</sup> A. Blandino, M. Macías and D. Cantero, *Enzyme Microb. Technol.*, **27**, 319 (2000), [https://doi.org/10.1016/S0141-0229\(00\)00204-0](https://doi.org/10.1016/S0141-0229(00)00204-0)
- <sup>18</sup> C. Bregni, J. Degrossi, R. García, M. C. Lamas, R. Firenstein *et al.*, *Ars Pharmaceut.*, **41**, 245 (2000), <http://hdl.handle.net/10481/28324>
- <sup>19</sup> N. Işıklan, *J. Appl. Polym. Sci.*, **99**, 1310 (2006), <https://doi.org/10.1002/app.22012>
- <sup>20</sup> H. Isawi, *Arab. J. Chem.*, **13**, 5691 (2020), <https://doi.org/10.1016/j.arabjc.2020.04.009>
- <sup>21</sup> Z. Zou, B. Zhang, X. Nie, Y. Cheng, Z. Hu *et al.*, *RSC Adv.*, **10**, 39722 (2020), <https://doi.org/10.1039/D0RA04316H>
- <sup>22</sup> S. Bashir, Y. Y. Teo, S. Ramesh and K. Ramesh, *Polymer*, **92**, 36 (2016), <https://doi.org/10.1016/j.polymer.2016.03.045>



- <sup>23</sup> M. Upadhyay, S. K. R. Adena, H. Vardhan, S. Pandey and B. Mishra, *Drug Dev. Ind. Pharm.*, **44**, 511 (2018), <https://doi.org/10.1080/03639045.2017.1402921>
- <sup>24</sup> R. V. Kulkarni, R. Boppana, G. K. Mohan, S. Mutalik and N. V. Kalyane, *J. Colloid Interface Sci.*, **367**, 509 (2012), <https://doi.org/10.1016/j.jcis.2011.10.025>
- <sup>25</sup> B. Niu, J. Jia, H. Wang, S. Chen, W. Cao *et al.*, *Int. J. Biol. Macromol.*, **141**, 1191 (2019), <https://doi.org/10.1016/j.ijbiomac.2019.09.059>
- <sup>26</sup> M. Palomo, M. Ballesteros and P. Frutos, *Drug Dev. Ind. Pharm.*, **23**, 273 (1997), <https://doi.org/10.3109/03639049709149804>
- <sup>27</sup> A. R. Sallmann, *Am. J. Med.*, **80**, 29 (1986), [https://doi.org/10.1016/0002-9343\(86\)90076-8](https://doi.org/10.1016/0002-9343(86)90076-8)
- <sup>28</sup> E. M. Elzayat, M. F. Ibrahim, A. A. Abdel-Rahman, S. M. Ahmed, F. K. Alanazi *et al.*, *Arab. J. Chem.*, **10**, S3245 (2017), <https://doi.org/10.1016/j.arabjc.2013.12.022>
- <sup>29</sup> A. Kumar, K. Singh and M. Ahuja, *Carbohydr. Polym.*, **76**, 261 (2009), <https://doi.org/10.1016/j.carbpol.2008.10.014>
- <sup>30</sup> R. Boppana, R. V. Kulkarni, G. K. Mohan, S. Mutalik and T. M. Aminabhavi, *RSC Adv.*, **6**, 64344 (2016), <https://doi.org/10.1039/C6RA04218J>
- <sup>31</sup> R. Boppana, G. K. Mohan, U. Nayak, S. Mutalik, B. Sa *et al.*, *Int. J. Biol. Macromol.*, **75**, 133 (2015), <https://doi.org/10.1016/j.ijbiomac.2015.01.029>
- <sup>32</sup> T. Hussain, T. Hussain and D. Gowda, *J. Young Pharm.*, **9**, 525 (2017), <https://doi.org/10.5530/jyp.2017.9.102>
- <sup>33</sup> M. N. Ghosh, *Indian J. Pharmacol.*, **39**, 216 (2007), [https://journals.lww.com/iphr/fulltext/2007/39040/fundamentals\\_of\\_experimental\\_pharmacology.13.aspx](https://journals.lww.com/iphr/fulltext/2007/39040/fundamentals_of_experimental_pharmacology.13.aspx)
- <sup>34</sup> C. A. Winter, E. A. Risley and G. W. Nuss, *Exp. Biol. Med.*, **111**, 544 (1962), <https://doi.org/10.3181/00379727-111-27849>
- <sup>35</sup> C. Liu, X. Dai, J. Chen, Y. Chen, X. Guo *et al.*, *J. Appl. Polym. Sci.*, **113**, 2339 (2009), <https://doi.org/10.1002/app.30305>
- <sup>36</sup> T. K. Giri, D. Thakur, A. Alexander, Ajazuddin, H. Badwaik *et al.*, *J. Mater. Sci.: Mater. Med.*, **24**, 1179 (2013), <https://doi.org/10.1007/s10856-013-4884-7>
- <sup>37</sup> U. S. Toti and T. M. Aminabhavi, *J. Control. Release*, **95**, 567 (2004), <https://doi.org/10.1016/j.jconrel.2003.12.019>
- <sup>38</sup> A. A. Ahmed, H. B. Naik and B. Sherigara, *Carbohydr. Res.*, **344**, 699 (2009), <https://doi.org/10.1016/j.carres.2009.01.011>
- <sup>39</sup> K. S. Soppirnath and T. M. Aminabhavi, *Eur. J. Pharm. Biopharm.*, **53**, 87 (2002), [https://doi.org/10.1016/S0939-6411\(01\)00205-3](https://doi.org/10.1016/S0939-6411(01)00205-3)
- <sup>40</sup> R. Boppana, R. V. Kulkarni, S. S. Mutalik, M. Setty and B. Sa, *J. Microencapsul.*, **27**, 337 (2010), <https://doi.org/10.3109/02652040903191842>
- <sup>41</sup> A. P. Rokhade, N. B. Shelke, S. A. Patil and T. M. Aminabhavi, *J. Microencapsul.*, **24**, 274 (2007), <https://doi.org/10.1080/02652040701281365>
- <sup>42</sup> S. A. Agnihotri, S. S. Jawalkar and T. M. Aminabhavi, *Eur. J. Pharm. Biopharm.*, **63**, 249 (2006), <https://doi.org/10.1016/j.ejpb.2005.12.008>
- <sup>43</sup> K. S. Soppimath, A. R. Kulkarni and T. M. Aminabhavi, *J. Control. Release*, **75**, 331 (2001), [https://doi.org/10.1016/S0168-3659\(01\)00404-7](https://doi.org/10.1016/S0168-3659(01)00404-7)
- <sup>44</sup> S. Kaity and A. Ghosh, *Int. J. Drug Deliv. Technol.*, **33**, 1 (2016), <https://doi.org/10.1016/j.jddst.2016.02.005>
- <sup>45</sup> S. Maiti, S. Ranjit, R. Mondol, S. Ray and B. Sa, *Carbohydr. Polym.*, **85**, 164 (2011), <https://doi.org/10.1016/j.carbpol.2011.02.010>